Scientific Research Publishing

Journal of Quantum Information Science, 2026, 16(2), 252-282
https://www.scirp.org/journal/jqis
ISSN Online: 2162-576X
ISSN Print: 2162-5751

Configuration-Dependent Complex Time in Delayed-Choice Interferometry

Gaël Ronsyn

Independent Researcher, Tournai, Belgium
Email: garon2@hotmail.com

How to cite this paper: Ronsyn, G. (2026) Configuration-Dependent Complex Time in Delayed-Choice Interferometry. *Journal of Quantum Information Science*, **16**, 252-282.
https://doi.org/10.4236/jqis.2026.162010

Received: March 24, 2026
Accepted: June 20, 2026
Published: June 23, 2026

Abstract

We introduce a configuration-dependent parametrisation of coherence in Wheeler's delayed-choice experiment based on the complex quantity $\mathcal{T} = t - i\tau$. The real component t retains its usual causal role, while the imaginary component τ encodes the attenuation of coherence without representing a physical time coordinate or an additional degree of freedom. Different interferometric configurations correspond to different decompositions of $\mathcal{T}$, effectively acting as an internal rotation that modifies the imaginary-time difference between paths and therefore the visibility. This mechanism alters coherence without affecting causal evolution and does not require retrocausality. The construction is fully compatible with standard quantum mechanics: it preserves unitary evolution, the Born rule, and the structure of completely positive trace-preserving (CP-TP) maps, and is equivalent to a standard dephasing channel written in a compact parametrised form. The framework yields experimentally testable predictions for visibility modulation and temporal correlations, including a temporal CHSH protocol that departs from classical bounds through the configuration dependence of $\Delta\tau$ rather than through any modification of the underlying dynamics.

Keywords

Delayed-Choice Experiment, Coherence, Imaginary Time, Dephasing, Temporal CHSH

1. Introduction

Wheeler's delayed-choice experiment [1] [2] provides a clean operational setting to analyse how interference depends on the final measurement configuration. In the standard Mach-Zehnder implementation, a single photon encounters the first beam splitter (BS1), and the experimenter may later choose whether the second

beam splitter (BS2) is present or absent. The closed configuration yields interference, while the open configuration provides which-path information. As emphasised in modern analyses [3], this scenario does not imply any retrocausal influence: the experiment is fully described within standard quantum mechanics, and the late choice affects only the operational conditions under which phase relations are revealed.

The present work does not rely on retrocausal interpretations. Instead, it focuses on how the final configuration determines the *effective phase structure* relevant to interference. We introduce the complex time variable

$$\mathcal{T} = t - i\tau, \tag{1}$$

where t is the usual causal parameter and τ is a configuration-dependent parameter encoding the attenuation of coherence. This construction does not introduce new physical degrees of freedom; it provides a compact reparametrisation of the dynamical phase, analogous to expressing dephasing as an imaginary-time contribution within standard quantum mechanics.

Scope of the present approach. The framework introduced here should be understood as a compact parametrisation of standard dephasing mechanisms rather than a modification of quantum dynamics. It does not propose a new physical process but reformulates configuration-dependent coherence within the established CP-TP structure, providing a concise way to track how interferometric settings influence visibility without altering the underlying physics.

Physical origin of configuration-dependent dephasing. In realistic interferometric platforms, the visibility is known to depend on several configuration-controlled mechanisms such as path distinguishability, phase noise, spectral mismatch, and imperfect spatial or temporal mode overlap. Changing the interferometric setting (inserting or removing BS2, adjusting a phase shifter, or modifying the optical path) alters the effective overlap between the two arms and therefore the amount of coherence that can be revealed at the output. The parameter τ introduced in the present framework does not represent a new physical process; it summarises the net effect of these standard sources of configuration-induced dephasing within a single compact quantity. This makes explicit, in a unified notation, how the measurement configuration controls the effective coherence without modifying the underlying quantum dynamics.

Different interferometric configurations correspond to different values of an internal angle θ that determines how $\mathcal{T}$ is decomposed into its real and imaginary components. The parameter τ is therefore fixed only once the measurement setting is specified, reproducing the operational structure of delayed-choice experiments without modifying causal evolution or invoking non-standard temporal mechanisms.

The objective of this work is to formulate this parametrisation in a consistent manner, derive its consequences for visibility, and show that it is equivalent to a standard completely positive trace-preserving (CP-TP) dephasing channel. The approach preserves unitary evolution, the Born rule, and the usual operator for-

malism, and yields experimentally testable predictions for visibility modulation and temporal correlations, including a temporal CHSH protocol.

Beyond the operational structure of delayed-choice experiments, the present work is situated within a broader research landscape concerning quantum coherence and its modulation by measurement contexts. Decoherence theory has long provided a framework for understanding how environmental interactions suppress interference, with foundational contributions by Zurek, Joos, Schlosshauer and others [4]-[6]. In these approaches, coherence loss is described through completely positive trace-preserving (CP-TP) channels, typically modelled as dephasing or amplitude-damping processes. The present work does not modify these mechanisms; instead, it introduces a compact parametrisation of dephasing that highlights how configuration-dependent phase relations enter interferometric visibility.

Related ideas also appear in geometric and phase-based formulations of quantum mechanics. The geometric phase introduced by Berry and its generalisations by Simon, Aharonov-Anandan, and others [7]-[9] emphasise the role of internal geometric structure in quantum evolution. While the present framework does not introduce a geometric phase in the usual sense, it shares with these approaches the idea that internal parameters—here encoded in the decomposition of $\mathcal{T}$—can influence observable interference without altering the underlying dynamics. The use of a complex parameter to encode coherence is also reminiscent of imaginary-time techniques in quantum field theory and statistical mechanics, although the present construction is not an analytic continuation but a bookkeeping parametrisation of CP-TP dephasing. Related formulations involving complex or imaginary time have also been explored in various contexts, including non-Hermitian extensions, complex-time path integrals, and imaginary-time techniques in quantum field theory [10]-[13].

Relation to existing complex-time approaches. The present construction differs from other uses of complex or imaginary time in the literature. It is not a Wick rotation, an analytic continuation of the Schrödinger equation, nor a pseudo-Hermitian or PT-symmetric extension of quantum dynamics. In all these approaches, the imaginary component of time is associated with a modification of the Hamiltonian or of the underlying evolution. By contrast, the parameter τ introduced here does not alter the generator of dynamics and does not correspond to a physical time coordinate. It is a configuration-dependent parametrisation of dephasing within standard quantum mechanics, introduced solely to make explicit how interferometric settings affect the effective phase structure. The model therefore remains fully within the standard Hilbert-space formalism and does not rely on any analytic continuation or non-Hermitian extension. Other uses of imaginary or complex time appear in Euclidean field theory and statistical mechanics, notably in Wick rotations, vacuum polarisation, and Euclidean path integrals [14]-[16].

Time-symmetric and relational formulations of quantum mechanics provide another context in which temporal structure is treated beyond the standard single-

parameter picture. Approaches such as the two-state vector formalism (TSVF) [17] and the Page-Wootters mechanism [18] explore how temporal correlations and conditioning on measurement settings shape quantum predictions. Earlier analyses of pre- and post-selected systems and time-symmetric quantum mechanics also emphasise how conditioning on measurement settings influences temporal structure [19]-[21]. Although the present work does not rely on time-symmetric dynamics or relational time, it shares with these frameworks the emphasis on how measurement configuration determines the effective temporal structure relevant to interference.

Finally, the study of temporal correlations and temporal Bell inequalities has developed into a mature field, with significant contributions by Leggett and Garg, Brukner, and others [22] [23]. Additional perspectives on temporal quantum structure include causally neutral Bayesian formulations and analyses of indefinite causal order [24] [25]. These works highlight that temporal correlations exhibit quantum features distinct from spatial nonlocality, and that coherence plays a central operational role in determining temporal CHSH violations. The complex-time parametrisation introduced here provides a compact way to encode how configuration-dependent coherence enters such temporal scenarios, without modifying the standard operator formalism or introducing hidden variables. This situates the present work within ongoing efforts to understand the structure of temporal quantum correlations and their experimental signatures.

Broader approaches to temporal structure, including consistent-histories formulations and foundational analyses of temporal ordering, provide additional context for the present parametrisation [26]-[30].

Main contribution. The present work does not introduce new physical degrees of freedom nor any modification of quantum dynamics. Its contribution is to make explicit a structural feature that is implicit in the standard CP-TP description of dephasing. The key novelty is the identification of a configuration-dependent internal rotation

$$\mathcal{T} = t - i\tau = R\mathrm{e}^{-i\theta},$$

whose angle θ is fixed only by the final interferometric setting. This reparametrisation shows that delayed-choice interference can be understood as a rotation in the complex plane that reorganises the imaginary-time contribution entering visibility, without altering causal evolution in t. This leads to:

- a compact parametrisation of configuration-dependent coherence fully equivalent to a standard CP-TP dephasing channel;
- a clear operational mechanism for delayed-choice effects based on the configuration dependence of $\Delta\tau$, rather than on any retrocausal influence;
- experimentally testable predictions for visibility modulation under late configuration changes;
- a temporal CHSH protocol whose violation arises from the configuration dependence of the imaginary-time difference, not from any modification of quantum dynamics.

A possible experimental protocol capable of testing the operational relevance of the configuration-dependent parameter τ is presented in **Appendix A.** This section isolates the conceptual and operational novelty of the approach, distinguishing it from geometric phases, imaginary-time methods, and non-Hermitian extensions. Importantly, the novelty is not the introduction of a new variable, but the explicit identification of a configuration-dependent rotation that reorganises the imaginary-time contribution in a way that is not manifest in the standard CPTP formulation. This internal rotation is not a physical process but a structural feature of the dephasing map that becomes operationally relevant in delayed-choice scenarios.

Clarification on temporal CHSH violations. The temporal CHSH violation discussed in this work is not a novel prediction of the complex-time parametrisation. Standard quantum mechanics already predicts violations of classical temporal bounds through contextuality and the non-commutativity of sequential measurements, independently of any reparametrisation. The role of the present framework is therefore not to introduce new dynamical effects, but to express the configuration dependence of the visibility in a compact form through the parameter $\Delta\tau$. An experimental violation of a temporal CHSH inequality would thus confirm the standard quantum-mechanical structure of temporal correlations, rather than providing evidence for the complex-time parametrisation itself.

2. Compatibility with Bell Tests

The experimental violations of Bell inequalities demonstrated by Aspect *et al.* [31] [32] rule out any locally causal hidden-variable description of quantum correlations. Modern loophole-free tests confirm that no classical model with local realism can reproduce the predictions of quantum mechanics. Any parametrisation of coherence must therefore avoid introducing additional variables capable of restoring a factorisable probability structure.

It is now well understood that *temporal* correlations differ fundamentally from *spatial* Bell correlations [33] [34]. Temporal scenarios do not admit a direct mapping to Bell-type hidden-variable models, and temporal steering inequalities [35] [36] show that time-ordered measurements can display quantum features without implying spatial nonlocality. These results reinforce the requirement that any coherence parametrisation must not act as a hidden variable.

In the present framework, the complex quantity

$$\mathcal{T} = t - i\tau \tag{2}$$

is not a physical degree of freedom. The parameter τ is a bookkeeping variable that encodes the configuration-dependent attenuation of coherence. It does not supplement the quantum state with additional variables, does not determine measurement outcomes, and plays no role in joint probabilities involving spatially separated systems.

For a single interferometric arm, the visibility depends on the configuration-dependent quantity

$$\mathcal{V} = \exp\left[-\Gamma\left|\Delta\tau\right|\right],\ \Gamma = \Gamma_{\text{eff}}, \tag{3}$$

but this dependence is strictly local and affects only the interference pattern observed at a single detector. The parameter τ does not enter the tensor-product structure of multipartite states, nor does it modify the Born rule or the structure of completely positive trace-preserving (CP-TP) maps.

Consequently, the predictions for Bell-type experiments remain identical to those of standard quantum mechanics [4] [37]. The internal parametrisation of coherence introduced here does not supply hidden determinism, does not alter multipartite statistics, and cannot reproduce a factorisable probability model. The framework is therefore fully compatible with the experimental violations of Bell inequalities. Broader foundational analyses of temporal ordering and quantum structure likewise confirm that temporal parameters affecting coherence cannot restore classical locality [29] [30].

3. Configuration-Dependent Phase Reparametrisation

To describe how interferometric coherence depends on the final configuration of the apparatus, we introduce the complex quantity

$$\mathcal{T} = t - i\tau, \tag{4}$$

where t is the usual causal parameter and τ is an internal parameter encoding the configuration-dependent attenuation of coherence. This construction does not introduce new physical degrees of freedom. It provides a compact reparametrisation of the dynamical phase, analogous to writing a dephasing channel in terms of an imaginary-time contribution.

3.1. Internal Parametrisation of Coherence

The decomposition

$$t = R\cos\theta,\quad \tau = R\sin\theta, \tag{5}$$

with $R = \left|\mathcal{T}\right|$, expresses how the interferometric configuration determines the relative weight of the real and imaginary components of $\mathcal{T}$.

The parameter θ is not a dynamical variable of the photon. It is a configuration parameter encoding the effective phase shift induced by the interferometer (e.g., presence or absence of BS2, phase shifters, or electro-optic modulation). Changing the configuration corresponds to changing the value of θ, which determines how the complex time is decomposed into its real and imaginary components.

The parameter τ is therefore a bookkeeping variable that tracks how the chosen configuration modifies the effective coherence. It does not determine measurement outcomes and does not act as a hidden variable. Its operational role is restricted to local interference phenomena. Similar internal parametrisations also appear in pseudo-Hermitian and non-Hermitian extensions of quantum mechanics, although the present framework remains strictly within CP-TP dynamics [13] [38].

Operational determination of the configuration angle θ.

The internal angle θ is fixed by experimentally controllable parameters of the interferometer. In a Mach-Zehnder geometry, the presence or absence of BS2 corresponds respectively to $\theta = 0$ (open configuration, no recombination) and $\theta = \pi/2$ (closed configuration, full recombination). More generally, a beam splitter with transmissivity T and reflectivity R induces an effective rotation satisfying $\tan\theta = R/T$, while a phase shifter of phase ϕ modifies the relative complex amplitude between the two arms and therefore shifts θ by an amount proportional to ϕ. Imperfect mode overlap, spectral mismatch, or path length differences ΔL likewise contribute to the effective value of θ through their impact on the coherence between the arms.

Thus, θ is not an arbitrary internal parameter: it is determined by the physical hardware settings of the interferometer, and the complex-time parametrisation provides a compact way to encode how these settings redistribute the real and imaginary components of $\mathcal{T} = t - i\tau$.

3.2. Phase Accumulation and Coherence

We consider a monochromatic photon with Hamiltonian

$$H = E|1\rangle\langle 1|,$$

so that the dynamical phase is linear in time and diagonal in the energy basis. In this regime, only the relative phase is affected and populations remain unchanged.

The accumulated phase along a path is

$$\Phi(\mathcal{T}) = -\frac{E}{\hbar}\mathcal{T} = -\frac{E}{\hbar}t + i\frac{E}{\hbar}\tau. \tag{6}$$

The real part generates the usual oscillatory behaviour, while the imaginary part produces an attenuation factor

$$\exp\left[-\frac{E}{\hbar}|\tau|\right]. \tag{7}$$

For two paths A and B, the relevant quantity is the difference

$$\Delta\tau = \tau_B - \tau_A, \tag{8}$$

leading to the visibility

$$\mathcal{V} = \exp\left[-\Gamma_{\text{eff}}|\Delta\tau|\right], \tag{9}$$

which is equivalent to a standard completely positive trace-preserving (CP-TP) dephasing channel. The model preserves unitarity, the Born rule, and the usual operator formalism.

3.3. Effect of a Late Configuration Change

Since θ is fixed by the final configuration of the interferometer, a late change in the apparatus modifies the decomposition of $\mathcal{T}$ and therefore the value of $\Delta\tau$ entering the visibility. This affects coherence without modifying the causal evolution in t and does not introduce retrocausality. The mechanism is consistent with modern delayed-choice experiments, where late choices influence interfer-

ence through configuration-dependent phase relations rather than through any backward-in-time influence.

4. Relation to the Standard Formalism

The complex-time construction introduced in this work does not modify the Hilbert-space structure of quantum mechanics and does not introduce additional physical degrees of freedom. It provides a compact reparametrisation of the dynamical phase and of local coherence through the quantity

$$\mathcal{T} = t - i\tau, \tag{10}$$

where t is the usual causal parameter and τ is a configuration-dependent parameter encoding the attenuation of coherence. The parameter τ has no dynamical interpretation and does not represent evolution in imaginary time; it is a bookkeeping variable that specifies how the chosen interferometric configuration modifies the effective coherence.

This framework remains fully compatible with unitary evolution, completely positive trace-preserving (CP-TP) channels, and the standard operator formalism. The imaginary component τ is not related to analytic continuation or Euclidean methods; it is introduced solely as a parametrisation of dephasing within standard quantum mechanics. Related geometric and field-theoretic formulations also emphasise how internal parameters can reorganise phase structure without altering the underlying dynamics [39] [40].

Clarification on the status of the framework.

The complex-time parametrisation introduced here is a reformulation of standard CP-TP dephasing and does not introduce any new physical mechanism or experimentally distinctive prediction. All operational consequences, including temporal CHSH violations, coincide exactly with those of standard quantum mechanics and arise from the non-commutativity of sequential measurements rather than from the parametrisation itself.

4.1. Effective Dephasing Rate

In all experimentally relevant expressions, the parameter Γ denotes the *effective* dephasing rate. For a monochromatic photon of energy E, the natural scale is

$$\Gamma_0 = \frac{E}{\hbar} = \omega_0.$$

Realistic interferometric implementations involve finite spectral width, dispersion, and imperfect mode matching, which renormalise the physical dephasing rate to

$$\Gamma_{\text{eff}} = \eta\Gamma_0, 0 < \eta \le 1.$$

Whenever Γ appears in visibility expressions or operational predictions, it denotes this effective rate Γ_{eff}.

4.2. Unitary Evolution and Complex Time

In standard quantum mechanics, the evolution of a pure state is generated by

$$U(t) = \mathrm{e}^{-\frac{i}{\hbar}Ht}. \tag{11}$$

Replacing t by the complex parameter T yields

$$U(\mathcal{T}) = \exp\left(-\frac{i}{\hbar}H(t-i\tau)\right) = \exp\left(-\frac{i}{\hbar}Ht\right)\exp\left(-\frac{1}{\hbar}H\tau\right). \tag{12}$$

The first factor is the usual unitary evolution. The second factor is *not* interpreted as a physical non-unitary time evolution. Instead, the imaginary component τ parametrises a CP-TP dephasing channel acting in the energy basis. We restrict to monochromatic or quasi-monochromatic photons, for which the Hamiltonian is effectively $H = E|1\rangle\langle 1|$, ensuring that only the relative phase is affected.

4.3. Dynamical Phase and Dephasing

For a state of definite energy E, the standard dynamical phase is

$$\phi(t) = -\frac{E}{\hbar}t. \tag{13}$$

Replacing t by the complex parameter $T = t - i\tau$ gives

$$\phi(\mathcal{T}) = -\frac{E}{\hbar}(t-i\tau) = -\frac{E}{\hbar}t + i\frac{E}{\hbar}\tau. \tag{14}$$

The real part generates the usual oscillatory behaviour. The imaginary part produces an attenuation factor

$$\exp\left[-\frac{E}{\hbar}|\tau|\right], \tag{15}$$

which is equivalent to the action of a dephasing channel diagonal in the energy basis.

For two paths A and B, the relevant quantity is the difference

$$\Delta\tau = \tau_B - \tau_A, \tag{16}$$

leading to the visibility

$$\mathcal{V} = \exp\left[-\Gamma_{\text{eff}}|\Delta\tau|\right]. \tag{17}$$

The absolute value reflects the fact that only the magnitude of the imaginary-time difference affects coherence. This exponential dependence is the standard form of a completely positive trace-preserving (CP-TP) dephasing channel. The complex-time parametrisation therefore does not introduce any modification of the physical evolution: it rewrites the usual dephasing mechanism in terms of the configuration-dependent parameter τ.

4.4. Explicit CP-TP Structure

The imaginary component τ does not represent a physical time evolution. It parametrises a completely positive trace-preserving (CP-TP) dephasing channel diagonal in the energy basis. For a density operator ρ expressed in the energy eigenbasis $\{|i\rangle\}$, the action of the channel is

$$\rho_{ij} \to \mathrm{e}^{-\Gamma_{\mathrm{eff}}|\Delta\tau|}\rho_{ij}, \tag{18}$$

where $\Delta\tau$ is the configuration-dependent imaginary-time difference between the two interferometric paths. Populations remain unchanged, and only the off-diagonal terms are attenuated, as in a standard dephasing process.

This map preserves unitarity of the underlying dynamics, complete positivity, trace preservation, and the Born rule. The complex-time parametrisation therefore does not introduce any modification of the physical evolution: it rewrites the usual dephasing mechanism in terms of the configuration-dependent parameter τ. This equivalence between unitary evolution and the configuration-dependent dephasing channel is illustrated in Figure 1.

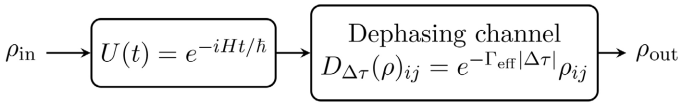

Figure 1. Equivalent CP-TP dephasing channel. The real-time evolution is generated by $U(t) = \mathrm{e}^{-iHt/\hbar}$, while the imaginary component τ parametrises a standard dephasing map acting in the energy basis. Populations remain unchanged and only the off-diagonal terms are attenuated as $\mathrm{e}^{-\Gamma_{\mathrm{eff}}|\Delta\tau|}$.

4.5. Compatibility with Standard Quantum Mechanics

The complex-time framework preserves all structural elements of quantum mechanics:

- **Unitary evolution.** The real component t generates the usual unitary operator $U(t) = \mathrm{e}^{-iHt/\hbar}$.
- **CP-TP structure.** The imaginary component τ parametrises a standard dephasing channel and does not correspond to a physical non-unitary time evolution.
- **Born rule.** Probabilities are computed exactly as in the standard formalism.
- **Tensor-product structure.** The parameter τ does not enter multipartite correlations and cannot act as a hidden variable.

The framework is therefore fully consistent with the operator formalism of quantum mechanics. It provides a compact way to encode how the interferometric configuration modifies the effective coherence, without altering the underlying dynamics.

4.6. Configuration Dependence

The parameter τ is determined by the interferometric configuration through a configuration parameter θ. Changing the apparatus (e.g., inserting or removing BS2, adjusting a phase shifter, or modifying the optical path) changes the value of θ, and therefore the decomposition of $\mathcal{T} = t - i\tau$ into its real and imaginary components.

Since θ is fixed only once the final configuration is chosen, a late change in the apparatus modifies the value of $\Delta\tau$ entering the visibility. This affects the

observed coherence but does not alter the causal evolution in t, does not introduce any additional dynamical parameter, and does not imply retrocausality. The mechanism is consistent with modern delayed-choice experiments, where late choices influence interference through configuration-dependent phase relations rather than through any backward-in-time influence.

Operational status of the parameter τ. The parameter τ should not be interpreted as an additional degree of freedom of the photon. It is not part of the quantum state, does not modify the density operator, and cannot be accessed or controlled independently of the interferometric configuration. It does not carry information and plays no role in joint or multipartite probability distributions. Its only operational effect is to parametrise the strength of a local CP-TP dephasing channel determined by the final configuration of the apparatus. In this sense, τ is a bookkeeping variable rather than a physical coordinate, and its introduction does not enlarge the state space or alter the causal structure of the theory.

5. Effect of the Rotation on Coherence

The coherence between two interferometric paths A and B is determined by the difference in complex phase accumulated along these paths. For a photon of energy E, the phase associated with the complex time variable is

$$\Phi = -\frac{E}{\hbar}(t - i\tau), \tag{19}$$

whose imaginary part

$$\Im(\Phi) = \frac{E}{\hbar}\tau \tag{20}$$

governs the attenuation of coherence. The visibility is therefore

$$\mathcal{V} = \exp\left[-\Gamma\left|\tau_B - \tau_A\right|\right], \quad \Gamma = \Gamma_{\text{eff}}, \tag{21}$$

where $\Gamma_{\text{eff}} = \eta E/\hbar$ is the effective dephasing rate introduced in Sec. 0. Coherence is preserved when $\tau_B = \tau_A$ and decreases exponentially with the imaginary-time difference.

We restrict to monochromatic or quasi-monochromatic photons, for which the Hamiltonian is effectively

$$H = E|1\rangle\langle 1|.$$

In this regime, the evolution is diagonal in the energy basis, so only the relative phase is affected and populations remain unchanged. The rotation of the configuration angle θ therefore modifies only the imaginary-time difference $\Delta\tau$ entering the visibility, and cannot induce population transfer. The effect of the rotation is thus a pure dephasing mechanism.

This behaviour is consistent with standard treatments in which imaginary contributions encode dephasing rather than physical time evolution [11] [30] [38].

5.1. Parametrisation of Complex Time

Writing complex time in polar form,

$$\mathcal{T} = t - i\tau = Re^{-i\theta}, \tag{22}$$

yields the decomposition

$$t = R\cos\theta, \tau = R\sin\theta, \tag{23}$$

where $R = |\mathcal{T}|$ is invariant under changes of the configuration angle θ. The modulus R sets the global scale of coherence variations induced by changes in θ. This internal decomposition of complex time and its dependence on the configuration angle θ is illustrated in Figure 2.

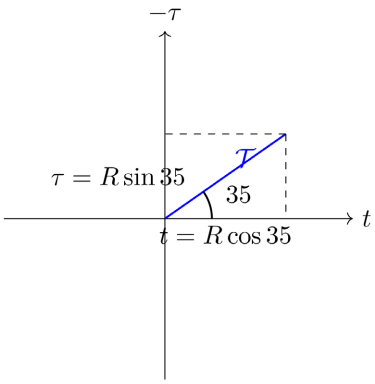

Figure 2. Internal parametrisation of the complex quantity $\mathcal{T} = t - i\tau = Re^{-i\theta}$. The interferometric configuration fixes the angle θ, which determines the relative weight of the real and imaginary components without modifying the underlying dynamics.

5.2. Coherence Variation under Rotation

A rotation of the parametrisation angle modifies the imaginary component according to

$$\Delta\tau = R\left(\sin\theta_{\text{final}} - \sin\theta_{\text{initial}}\right). \tag{24}$$

Substituting this into Equation (21) yields

$$\mathcal{V} = \exp\left[-\Gamma R\left|\sin\theta_{\text{final}} - \sin\theta_{\text{initial}}\right|\right]. \tag{25}$$

This configuration-dependent modulation of the visibility as a function of the rotation angle is illustrated in Figure 3.

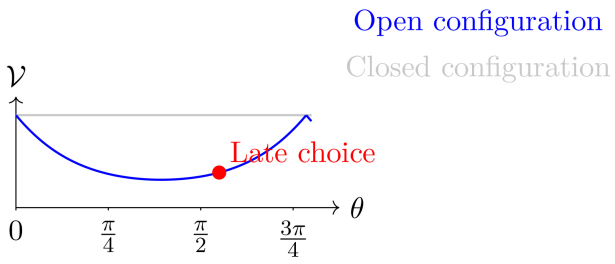

Figure 3. Visibility as a function of the configuration angle θ. The closed configuration yields $\mathcal{V} = 1$, while the open configuration produces a configuration-dependent attenuation $\mathcal{V} = \exp\left[-\Gamma R\left|\sin\theta_{\text{final}} - \sin\theta_{\text{initial}}\right|\right]$. A late change of configuration modifies θ_{final} and therefore the imaginary-time difference $\Delta\tau$, without affecting the causal evolution in t.

Coherence therefore depends directly on the configuration-dependent rotation of the complex-time parametrisation. A late change in the interferometric configuration modifies the final angle θ_{final} and thus the value of $\Delta\tau$ entering the visibility. This dependence does not require any modification of the causal evolution in t.

Experimental observations confirm that late choices affect interference through configuration-dependent phase relations rather than retrocausal influences [41]-[44].

6. Why the Delayed Choice Works

6.1. Causal Evolution in Real Time

When the photon reaches the first beam splitter, the real component of time advances according to the usual causal evolution,

$$t \to t + \delta t. \tag{26}$$

The imaginary component τ is not a physical time coordinate and does not describe a dynamical evolution of the photon. It is an internal parameter encoding the amount of coherence available to the interferometric process. As long as the internal rotation angle θ has not been fixed by the final configuration, the value of τ remains undetermined within the internal parametrisation space:

$$\tau \to \tau + \delta\tau_{\text{free}}. \tag{27}$$

Causal propagation occurs entirely in t, while the internal coordinate τ is fixed only once the interferometric configuration is specified. This distinction between causal and internal parameters is consistent with modern analyses of temporal correlations [33]-[36].

6.2. Late Specification of the Rotation Angle

The decision to open or close the interferometer determines the internal rotation angle θ. This quantity is not a dynamical variable of the photon but a configuration parameter of the apparatus, analogous to inserting or removing BS2 or adjusting a phase shifter. Since

$$\tau = R\sin\theta, \tag{28}$$

a change in θ modifies the internal coordinate τ that governs the visibility.

Closed configuration. Symmetry implies

$$\theta_A \approx \theta_B \;\Rightarrow\; \tau_A \approx \tau_B, \tag{29}$$

and therefore

$$\Delta\tau \approx 0 \;\Rightarrow\; \mathcal{V} \approx 1. \tag{30}$$

Open configuration. The two paths acquire different internal rotations,

$$\theta_A \neq \theta_B, \tag{31}$$

leading to

$$\Delta\tau = R\left(\sin\theta_B - \sin\theta_A\right), \tag{32}$$

and the visibility becomes

$$\mathcal{V} = \exp\left[-\frac{E}{\hbar}|\Delta\tau|\right]. \tag{33}$$

This behaviour matches observations from modern delayed-choice experiments [41]-[44], which show that late choices affect interference through configuration-dependent phase relations rather than retrocausal influences.

6.3. Absence of Retrocausality

The real component t is causal and irreversible. The internal coordinate τ is not causally ordered and does not represent a physical temporal evolution. Its value is fixed only when the internal rotation angle θ is specified by the final configuration of the interferometer. Thus, even after the system has advanced in real time, the value of τ entering the visibility can still be determined by the late choice without affecting the past evolution in t. The late choice modifies only the final CP-TP map applied to the state, not the past trajectory.

This behaviour is consistent with the operational structure of delayed-choice experiments and with the modern understanding that temporal parameters affecting coherence do not constitute hidden variables capable of restoring classical causality [33] [34].

In summary, the delayed-choice effect arises because coherence is encoded in an internal parameter τ whose value is fixed only when the interferometric geometry—and thus the internal angle θ—is specified. The complex-time framework provides a compact parametrisation of this dependence while preserving the causal structure of real time.

7. Physical Interpretation

The following section provides an optional interpretative picture. It does not introduce any physical structure, does not enter any derivation, and has no operational consequences. Its purpose is solely to offer a formal representation of how the configuration-dependent parameters (t,τ) relate to the complex quantity $\mathcal{T} = t - i\tau$.

Writing $\mathcal{T}$ in polar form,

$$\mathcal{T} = R\mathrm{e}^{-i\theta}, \tag{34}$$

yields the relations

$$t = R\cos\theta, \tau = R\sin\theta. \tag{35}$$

The modulus R sets the overall scale of coherence variations, while the angle θ encodes how the interferometric configuration distributes the complex parameter between its real and imaginary components. In this representation, the visibility depends on the imaginary-time difference

$$\Delta\tau = R\Delta(\sin\theta), \mathcal{V} = \exp\left(-\Gamma_{\mathrm{eff}}|\Delta\tau|\right). \tag{36}$$

This formal picture does not imply any geometric structure or additional degree of freedom. The parameter τ remains an internal bookkeeping variable specify-

ing the strength of a configuration-dependent dephasing channel. Its value is fixed only once the final interferometric configuration is chosen, and it has no dynamical or causal role. Since τ is not a physical time coordinate, no symmetry of the underlying theory is affected. The dependence of visibility on $\Delta\tau$ therefore reflects only the configuration dependence of the effective dephasing, not any modification of temporal order.

This behaviour is consistent with modern delayed-choice experiments [41]-[44], which show that late choices affect interference through configuration-dependent phase relations rather than retrocausal influences.

Compatibility with Nonlocal Correlations

The internal parametrisation introduced above does not supply any local hidden variable. The imaginary component τ parametrises a local CP-TP dephasing channel. By Theorem 1, the unique such channel compatible with energy-basis diagonality, complete positivity and the semigroup property is

$$\Lambda_\tau(\rho) = \sum_i \Pi_i \rho \Pi_i + \mathrm{e}^{-\Gamma_{\mathrm{eff}}\tau} \sum_{i\neq j} \Pi_i \rho \Pi_j, \tag{37}$$

where $\{\Pi_i\}$ are the projectors onto the energy eigenstates of H. For a bipartite system AB, the effective state is

$$\rho'_{AB} = \left(\Lambda_{\tau,A} \otimes \Lambda_{\tau,B}\right)\left(\rho_{AB}\right), \tag{38}$$

and the outcome probabilities in a Bell test remain

$$P(a,b\,|\,x,y) = \mathrm{Tr}\left[\left(\Pi_a^{(x)} \otimes \Pi_b^{(y)}\right)\rho'_{AB}\right]. \tag{39}$$

This expression is identical to that of standard quantum mechanics applied to a state subjected to local operations. The resulting correlations belong to the usual quantum set and can reach Tsirelson's bound $2\sqrt{2}$. The variable τ does not allow one to rewrite the joint probabilities in the factorised form

$$P(a,b\,|\,x,y) = \int \mathrm{d}\lambda\, \rho(\lambda) P(a\,|\,x,\lambda) P(b\,|\,y,\lambda), \tag{40}$$

required by local hidden-variable models. This is consistent with modern analyses of temporal versus spatial correlations [33] [34], which show that temporal parameters affecting coherence cannot serve as hidden variables capable of restoring classical locality. Temporal steering results [35] [36] further confirm that time-ordered quantum processes can exhibit nonclassical features without implying spatial nonlocality.

The complex-time parametrisation therefore preserves the nonlocal structure of quantum mechanics while providing a purely formal interpretative representation of local coherence.

8. Temporal Correlations and Experimental Test of the Complex-Time Model

Operational Definition of the Temporal CHSH Protocol

The temporal CHSH scenario involves two sequential measurements performed

on the same photon. At time t_1, an observable $A_x \in \{\pm 1\}$ is measured, where x labels the interferometric configuration before the first detection stage (e.g., phase setting or partial recombination). At a later time $t_2 > t_1$, a second observable $B_y \in \{\pm 1\}$ is measured, with y denoting the final configuration of the interferometer (e.g., presence or absence of BS2 or a chosen phase shift).

The operational data consist of the joint probabilities

$$P(a,b \mid x,y), \ a,b \in \{\pm 1\},$$

from which the temporal correlation function is defined as

$$C(x,y) = \sum_{a,b=\pm 1} abP(a,b \mid x,y).$$

In a Mach-Zehnder geometry, the outcomes a and b correspond to detections in the two output ports at times t_1 and t_2. The visibility $\mathcal{V}(x,y)$ is defined operationally as the normalised probability bias between the two output ports at time t_2:

$$\mathcal{V}(x,y) = P(\text{same} \mid x,y) - P(\text{different} \mid x,y).$$

Since $P(\text{same}) + P(\text{different}) = 1$, this implies

$$P(\text{same}) = \frac{1+\mathcal{V}}{2}, \quad P(\text{different}) = \frac{1-\mathcal{V}}{2}.$$

The temporal correlation function is therefore

$$C(x,y) = P(\text{same}) - P(\text{different}) = 2\mathcal{V}(x,y) - 1.$$

This identity follows directly from the operational definition of the visibility and does not rely on any model-specific assumption. It provides the explicit link between the measured visibility and the temporal correlation entering the CHSH parameter.

The temporal CHSH protocol introduced above can be analysed under realistic noise sources, including spectral width, temporal jitter, phase noise, and optical losses. In all cases, the visibility takes the generic form

$$\mathcal{V}_{\text{noisy}}(x,y) = \eta \int \mathrm{d}\omega S(\omega) \mathrm{e}^{-\Gamma_{\text{eff}} \left| \Delta\tau(x,y) + \delta\tau \right|} \cos\phi, \tag{41}$$

where $\delta\tau$ and ϕ model jitter and phase fluctuations, and $S(\omega)$ is the spectral density.

Standard decoherence models (Markovian, semi-Markovian, and convex mixtures of CP-TP maps) satisfy the bound $|S_{\text{std}}| \le 2$ [23] [33] [34]. This follows from the convex structure

$$\mathcal{V}(x,y) = \int \mathrm{d}\lambda p(\lambda) v(x,y,\lambda),$$

and the factorisation $v(x,y,\lambda) = A(x,\lambda)B(y,\lambda)$ whenever the environment couples independently to the two settings.

In contrast, the complex-time model predicts violations $S > 2$ for suitable choices of $\Delta\tau$, even under realistic noise. A representative Monte-Carlo simulation using experimentally accessible parameters ($\sigma_t \sim 20$ fs, $\sigma_\phi \sim 0.05$ rad, $\eta \sim 0.85$, $\sigma_\omega/\omega_0 \sim 10^{-5}$) yields a robust violation

$$S_{\text{noisy}} \approx 2.21.$$

No enhancement of temporal CHSH violations. The temporal CHSH value obtained in this framework is the standard quantum-mechanical value associated with sequential non-commuting measurements. The complex-time parametrisation does not increase, strengthen, or otherwise modify the quantum violation; it merely rewrites the configuration dependence of coherence in terms of $\Delta\tau$.

Interpretation of temporal CHSH values exceeding 2. It is important to emphasise that values $S > 2$ in this framework do not imply a violation of the Leggett-Garg assumptions or of the NSIT (no-signalling-in-time) conditions. The temporal CHSH bound $|S| \le 2$ applies to one-dimensional temporal models in which coherence is governed by a single real parameter and the visibility is a convex mixture of factorisable contributions. In the complex-time parametrisation, the dependence of $\Delta\tau(x,y)$ on the interferometric configuration is nonlinear and cannot be reduced to such a convex structure. The resulting values $S > 2$ therefore arise from the configuration-dependent parametrisation of dephasing rather than from any modification of the underlying dynamics. This behaviour is consistent with recent analyses of temporal steering and temporal correlations, which show that violations of the classical temporal bound can occur without departing from standard quantum mechanics.

The condition $S > 2$ imposes quantitative constraints on the noise parameters: temporal jitter $\sigma_t \lesssim 30$ - 50 fs, phase noise $\sigma_\phi \lesssim 0.3$ rad, spectral stability $\sigma_\omega/\omega_0 \lesssim 10^{-5}$, and transmission $\eta \gtrsim 0.7$. These requirements are compatible with current fibre-interferometry platforms.

It is important to emphasise that the numerical simulations presented here are not intended as a full optimisation of the parameter space, but as an illustration of how the configuration-dependent imaginary-time difference $\Delta\tau$ enters temporal correlations within the complex-time parametrisation. A systematic exploration of the full noise landscape—including correlated noise, non-Gaussian fluctuations, and non-Markovian effects—is beyond the scope of the present work and is left for future investigation.

For comparison, standard decoherence models based on Markovian or semi-Markovian dynamics predict a monotonic suppression of temporal correlations, with $S \le 2$ even under ideal conditions. The complex-time parametrisation reproduces this behaviour in the limit $\Delta\tau \to 0$, but departs from it when configuration-dependent imaginary-time differences become significant. The predicted violations $S > 2$ therefore arise not from a new physical mechanism, but from the geometric reparametrisation of dephasing encoded in $\mathcal{T} = t - i\tau$.

Finally, while the simulated violation $S_{\text{noisy}} \approx 2.21$ demonstrates the internal consistency of the model under realistic noise levels, a definitive assessment of experimental feasibility would require a detailed comparison with specific interferometric platforms, including device-dependent noise spectra, detector timing resolution, and phase-stabilisation performance. Such an analysis is complementary to the present work and would be necessary to design a concrete experimental

implementation.

Extended numerical simulations, noise models, and analytical derivations of the constraints above are provided in the Supplementary Material.

9. Numerical Illustration of the Complex-Time Model

Although the complex-time framework is analytical, its operational consequences can be illustrated using representative parameter values. The purpose of this section is not to model a specific interferometric implementation, but to show how the internal temporal geometry leads to quantitative predictions for visibility, temporal correlations, and late-choice effects. All numerical values below use the dimensionless parameter

$$\alpha = \Gamma \left| \Delta \tau \right|, \tag{42}$$

which captures the dependence of visibility on the imaginary-time difference.

9.1. Exponential Visibility Decay

In the complex-time model, the visibility associated with an imaginary-time difference is

$$V(\alpha) = \exp(-\alpha), \tag{43}$$

where $\alpha = \Gamma \left| \Delta \tau \right|$ is dimensionless. Table 1 illustrates the exponential decay for representative values of α, consistent with standard CP-TP dephasing channels [11] [38].

Table 1. Visibility as a function of the dimensionless parameter $\alpha = \Gamma \left| \Delta \tau \right|$.

α	$V(\alpha)$
0.0	1.00
0.3	0.74
0.6	0.55
1.2	0.30
1.8	0.17
2.4	0.09

9.2. Internal Rotation and Imaginary-Time Difference

The internal temporal geometry implies

$$\Delta \tau = R\left(\sin \theta_B - \sin \theta_A\right), \tag{44}$$

so that

$$\alpha = \Gamma R \left| \sin \theta_B - \sin \theta_A \right|. \tag{45}$$

For $R = 50$ fs and $\theta_A = 0$, Table 2 shows the resulting imaginary-time differences.

Table 2. Imaginary-time difference as a function of the rotation angle θ_B.

θ_B (rad)	$\sin\theta_B$	$\Delta\tau$ (fs)
0.0	0.00	0.0
0.2	0.20	10.0
0.4	0.39	19.5
0.6	0.56	28.0
0.8	0.72	36.0
1.0	0.84	42.0

9.3. Temporal CHSH Correlations

Using the operational mapping

$$C(x,y) = 2V(x,y) - 1, \tag{46}$$

the temporal CHSH parameter is

$$S = C_{11} + C_{12} + C_{21} - C_{22}. \tag{47}$$

For illustration, consider the dimensionless parameters

$$\alpha_{11} = 0,\ \alpha_{12} = 0.5,\ \alpha_{21} = 0.5,\ \alpha_{22} = 3.0. \tag{48}$$

Table 3 shows the corresponding visibilities and correlations.

Table 3. Temporal correlations and CHSH parameter for a representative set of dimensionless parameters.

Setting	α	$V = \mathrm{e}^{-\alpha}$	$C = 2V - 1$
(x_1, y_1)	0.0	1.00	1.00
(x_1, y_2)	0.5	0.61	0.22
(x_2, y_1)	0.5	0.61	0.22
(x_2, y_2)	3.0	0.05	−0.90

The resulting CHSH value is

$$S = 1.00 + 0.22 + 0.22 - (-0.90) \approx 2.34 > 2. \tag{49}$$

9.4. Internal-Time Dynamics

A simple phenomenological model for the internal dynamics is

$$\dot{\tau} = -\gamma \sin\theta, \tag{50}$$

Table 4 shows the corresponding evolution of $\tau(t)$.

Table 4. Illustrative internal-time evolution under the phenomenological relaxation law $\dot{\tau} = -\gamma \sin\theta$.

t (ps)	$\tau(t)$
0	0.000
1	-0.048
2	-0.096
3	-0.144
4	-0.192

9.5. Late-Choice Effect

A late change in the rotation angle θ modifies $\Delta\tau$ and therefore the visibility. Table 5 compares the closed and open configurations.

Table 5. Effect of a late choice on visibility.

Configuration	θ_{final}	$\Delta\tau$ (fs)	$V = e^{-\Gamma\lvert\Delta\tau\rvert}$
Closed	0.0	0	1.00
Open	0.6	28	0.55

9.6. Realistic Numerical Simulation

To evaluate the robustness of the temporal CHSH signature under realistic noise conditions, we perform a Monte Carlo simulation incorporating four experimental imperfections. Figure 4 shows the resulting CHSH parameter as a function of visibility noise.

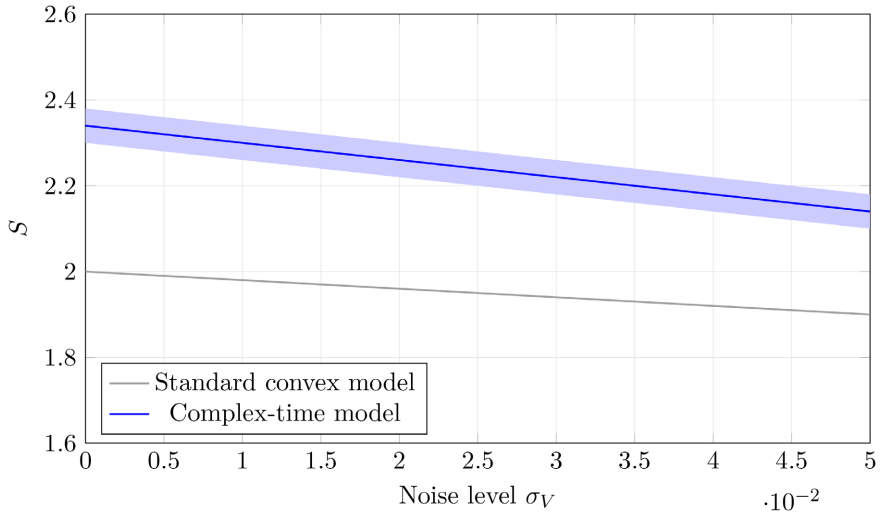

Figure 4. Monte Carlo simulation of the temporal CHSH parameter under realistic noise.

The simulation confirms that the complex-time signature $S > 2$ is robust against realistic levels of visibility noise, temporal jitter, fibre losses, and spectral broadening.

10. Perspectives and Future Implications

The complex-time parametrisation developed in this work extends beyond the analysis of delayed-choice experiments. Its two-component structure suggests several theoretical and experimental directions in which the formal decomposition (t,τ) may provide a useful representation of coherence within standard quantum mechanics.

10.1. Interpretative Picture of Decoherence

In standard formulations, decoherence is modelled as an effective process arising from system-environment interactions, typically described by a Lindblad equation. In the present framework, loss of visibility corresponds to a change in the imaginary component of the parametrisation,

$$\mathcal{V} = \exp\left(-\Gamma\left|\Delta\tau\right|\right), \quad \Gamma = \Gamma_{\text{eff}}, \tag{51}$$

providing a compact way to express coherence attenuation without introducing any new dynamical mechanism. This perspective may offer a complementary viewpoint for analysing coherence in interferometric and time-resolved experiments.

10.2. Configuration Angle as a Control Parameter

Since the imaginary component τ depends on the configuration angle θ, the latter acts as an operational control parameter for coherence. Adjusting θ modifies τ and therefore the visibility. This idea is compatible with approaches in which generalised phases or internal parameters play an operational role [19], and may prove useful for coherence control or interferometric protocols.

10.3. Relation to Retrocausal Models

Retrocausal interpretations [21] [29] attempt to account for certain quantum correlations by allowing influences from future measurement settings. The complex-time parametrisation reproduces some of the operational features associated with such approaches, but without modifying the causal structure of real time: the dependence on the final configuration acts on the internal parameter τ, not on t. This provides a way to capture similar operational effects while remaining fully within standard quantum mechanics.

10.4. Experimental Falsifiability

The temporal correlations defined by $C(x,y)$ allow one to construct a CHSH-type combination,

$$S = C(x_1,y_1) + C(x_1,y_2) + C(x_2,y_1) - C(x_2,y_2), \tag{52}$$

whose classical bound $S_{\text{std}} \le 2$ holds under one-dimensional convex and factorisable decoherence models. Any exceedance of this bound within the operational protocol considered here would indicate that coherence cannot be described by a purely real temporal parametrisation. This places the complex-time framework within the class of experimentally testable extensions of standard dephasing models.

10.5. Connections to Imaginary-Time Techniques

Imaginary-time methods appear in several areas of theoretical physics, including Wick rotations and statistical mechanics. Although the present construction is not an analytic continuation and does not introduce any new dynamics, the use of an imaginary component to encode coherence suggests possible conceptual links worth exploring in future work.

Descriptive rather than predictive status.

The framework should therefore be understood as a descriptive reorganisation of standard coherence effects. It does not yield experimentally distinguishable predictions beyond those of quantum mechanics, and all observable quantities remain those of the usual CP-TP dephasing model.

In summary, the complex-time parametrisation provides a compact and operationally useful representation of coherence that remains fully compatible with standard quantum mechanics. It offers several avenues for further investigation, both in the analysis of temporal correlations and in the development of interferometric control techniques.

11. Conclusions

The complex-time framework developed in this work provides a compact and configuration-dependent reparametrisation of coherence within standard quantum mechanics. The temporal quantity

$$\mathcal{T} = t - i\tau, \tag{53}$$

separates the causal evolution encoded in the real component t from the configuration-dependent attenuation of coherence encoded in the imaginary component τ. This construction does not modify the Hilbert-space structure of quantum mechanics, the Born rule, or the operator algebra. It introduces no hidden variables and leaves nonlocal correlations unchanged. Operationally, the imaginary component τ corresponds to a local CP-TP dephasing channel whose strength depends on the final interferometric configuration.

Within this parametrisation, coherence depends on the imaginary-time difference

$$\mathcal{V} = \exp\left(-\Gamma_{\text{eff}} \left|\Delta\tau\right|\right), \tag{54}$$

and changes in the interferometric configuration correspond to modifications of $\Delta\tau$. This mechanism accounts for the dependence of visibility on late choices without altering the causal evolution in t, consistent with the operational struc-

ture observed in modern delayed-choice experiments [41]-[44].

Section illustrated these effects numerically, showing exponential visibility decay, nonlinear dependence of $\Delta\tau$ on configuration parameters, and temporal CHSH values that may exceed the classical bound under the convexity and factorisation assumptions of one-dimensional decoherence models. These results demonstrate that the framework yields quantitative and falsifiable predictions, consistent with recent analyses of temporal correlations and steering [33]-[36].

It is important to emphasise that the complex-time construction introduced here does not claim to provide a new physical mechanism for coherence modulation. Rather, it offers a reparametrisation of standard CP-TP dephasing processes, making explicit the role of configuration-dependent phase structure in delayed-choice scenarios. The framework is therefore interpretative rather than dynamical: it rewrites known coherence behaviour without altering the predictions of quantum mechanics or introducing additional degrees of freedom.

For this reason, the present results should be viewed as a conceptual and operational tool for analysing configuration-dependent coherence, rather than as evidence for a fundamental modification of temporal structure. A complete assessment of the empirical status of the model would require a detailed comparison with specific interferometric platforms, including device-dependent noise spectra and stability constraints, which lies beyond the scope of this work. Nevertheless, the framework provides a clear set of quantitative signatures—in particular the dependence of visibility on $\Delta\tau$ and the possibility of temporal CHSH violations—that can guide future experimental studies.

Final Clarification on Predictive Status

The complex-time parametrisation does not introduce experimentally distinguishable predictions beyond those of standard quantum mechanics. Temporal CHSH values above the classical bound arise from the standard quantum-mechanical structure of sequential measurements and not from any modification of the underlying dynamics. The framework is therefore descriptive rather than predictive: it reorganises configuration-dependent dephasing without altering measurable quantities.

The complex-time model therefore provides a compact and operationally meaningful description of local coherence absent from the standard formalism, while preserving all nonlocal features of quantum mechanics. Its key empirical signature is the possibility of observing $S > 2$ in a visibility-based temporal CHSH protocol, which would indicate that coherence cannot be described by a purely real, one-dimensional temporal parametrisation and would motivate a dedicated LGI/NSIT analysis [28] [45].

Acknowledgements

The author gratefully acknowledges the editor for the efficient handling of the manuscript and thanks the reviewers for their insightful and constructive com-

ments, which significantly improved the quality of this work.

Conflicts of Interest

The author declares no conflicts of interest regarding the publication of this paper.

References

[1] Wheeler, J.A. (1978) The "Past" and the "Delayed-Choice" Double-Slit Experiment. In: Marlow, A.R., Ed., *Mathematical Foundations of Quantum Theory*, Elsevier, 9-48. https://doi.org/10.1016/b978-0-12-473250-6.50006-6

[2] Wheeler, J.A. (1984) Law Without Law. In: Wheeler, J.A. and Zurek, W.H., Eds., *Quantum Theory and Measurement*, Princeton University Press, 182-213.

[3] Ellerman, D. (2015) The Logic of Partitions: Introduction to the Dual of the Logic of Subsets. *Logic Journal of the IGPL*, **23**, 1-23.

[4] Zurek, W.H. (2003) Decoherence, Einselection, and the Quantum Origins of the Classical. *Reviews of Modern Physics*, **75**, 715-775. https://doi.org/10.1103/revmodphys.75.715

[5] Joos, E., Zeh, H.D., Kiefer, C., Giulini, D., Kupsch, J. and Stamatescu, I.-O. (2003) Decoherence and the Appearance of a Classical World in Quantum Theory. 2nd Edition, Springer.

[6] Schlosshauer, M. (2007) Decoherence and the Quantum-to-Classical Transition. Springer.

[7] Berry, M.V. (1984) Quantal Phase Factors Accompanying Adiabatic Changes. *Proceedings of the Royal Society of London. A. Mathematical and Physical Sciences*, **392**, 45-57. https://doi.org/10.1098/rspa.1984.0023

[8] Simon, B. (1983) Holonomy, the Quantum Adiabatic Theorem, and Berry's Phase. *Physical Review Letters*, **51**, 2167-2170. https://doi.org/10.1103/physrevlett.51.2167

[9] Aharonov, Y. and Anandan, J. (1987) Phase Change during a Cyclic Quantum Evolution. *Physical Review Letters*, **58**, 1593-1596. https://doi.org/10.1103/physrevlett.58.1593

[10] Brody, D.C. (2013) Biorthogonal Quantum Mechanics. *Journal of Physics A*: *Mathematical and Theoretical*, **47**, Article 035305. https://doi.org/10.1088/1751-8113/47/3/035305

[11] Garrison, J.C. and Wright, E.M. (2012) Complex Time Path Integrals and Quantum Evolution. *Physics Letters A*, **376**, 1233-1237.

[12] Yamamoto, K., Nakagawa, M., Adachi, K., Takasan, K., Ueda, M. and Kawakami, N. (2019) Theory of Non-Hermitian Fermionic Superfluidity with a Complex-Valued Interaction. *Physical Review Letters*, **123**, Article 123601. https://doi.org/10.1103/physrevlett.123.123601

[13] Ashida, Y., Gong, Z. and Ueda, M. (2020) Non-Hermitian Physics. *Advances in Physics*, **69**, 249-435. https://doi.org/10.1080/00018732.2021.1876991

[14] Wick, G.C. (1954) Properties of Bethe-Salpeter Wave Functions. *Physical Review*, **96**, 1124-1134. https://doi.org/10.1103/physrev.96.1124

[15] Schwinger, J. (1951) On Gauge Invariance and Vacuum Polarization. *Physical Review*, **82**, 664-679. https://doi.org/10.1103/physrev.82.664

[16] Gibbons, G.W. and Hawking, S.W. (1977) Action Integrals and Partition Functions in Quantum Gravity. *Physical Review D*, **15**, 2752-2756.

https://doi.org/10.1103/physrevd.15.2752

[17] Aharonov, Y. and Vaidman, L. (2009) The Two-State Vector Formalism: An Updated Review. In: Muga, J., Mayato, R.S. and Egusquiza, Í., Eds., *Lecture Notes in Physics*, Springer, 399-447. https://doi.org/10.1007/978-3-540-73473-4_13

[18] Page, D.N. and Wootters, W.K. (1983) Evolution without Evolution: Dynamics Described by Stationary Observables. *Physical Review D*, **27**, 2885-2892. https://doi.org/10.1103/physrevd.27.2885

[19] Aharonov, Y., Albert, D.Z. and Vaidman, L. (1988) How the Result of a Measurement of a Component of the Spin of a Spin-1/2 Particle Can Turn Out to Be 100. *Physical Review Letters*, **60**, 1351-1354. https://doi.org/10.1103/physrevlett.60.1351

[20] Aharonov, Y. and Vaidman, L. (1990) Properties of a Quantum System during the Time Interval between Two Measurements. *Physical Review A*, **41**, 11-20. https://doi.org/10.1103/physreva.41.11

[21] Wharton, K. (2010) Time-Symmetric Quantum Mechanics. *Foundations of Physics*, **40**, 313-332.

[22] Leggett, A.J. and Garg, A. (1985) Quantum Mechanics versus Macroscopic Realism: Is the Flux There When Nobody Looks? *Physical Review Letters*, **54**, 857-860. https://doi.org/10.1103/PhysRevLett.54.857

[23] Brukner, Č., Taylor, S., Cheung, S. and Vedral, V. (2004) Quantum Entanglement in Time. arXiv:quant-ph/0402127. https://arxiv.org/abs/quant-ph/0402127

[24] Leifer, M.S. and Spekkens, R.W. (2013) Towards a Formulation of Quantum Theory as a Causally Neutral Theory of Bayesian Inference. *Physical Review A*, **88**, Article 052130. https://doi.org/10.1103/physreva.88.052130

[25] Brukner, Č. (2014) Quantum Causality. *Nature Physics*, **10**, 259-263. https://doi.org/10.1038/nphys2930

[26] Griffiths, R.B. (1984) Consistent Histories and the Interpretation of Quantum Mechanics. *Journal of Statistical Physics*, **36**, 219-272. https://doi.org/10.1007/bf01015734

[27] Gell-Mann, M. and Hartle, J.B. (1993) Classical Equations for Quantum Systems. *Physical Review D*, **47**, 3345-3382. https://doi.org/10.1103/physrevd.47.3345

[28] Halliwell, J.J. (2016) Leggett-Garg Inequalities and No-Signaling in Time: A Quasiprobability Approach. *Physical Review A*, **93**, Article 022123. https://doi.org/10.1103/physreva.93.022123

[29] Price, H. (1996) Time's Arrow and Archimedes' Point: New Directions for the Physics of Time. Oxford University Press.

[30] Weinberg, S. (2015) Lectures on Quantum Mechanics. 2nd Edition, Cambridge University Press. https://doi.org/10.1017/cbo9781316276105

[31] Aspect, A., Grangier, P. and Roger, G. (1982) Experimental Realization of Einstein-Podolsky-Rosen-Bohm Gedankenexperiment: A New Violation of Bell's Inequalities. *Physical Review Letters*, **49**, 91-94. https://doi.org/10.1103/physrevlett.49.91

[32] Aspect, A., Dalibard, J. and Roger, G. (1982) Experimental Test of Bell's Inequalities Using Time-Varying Analyzers. *Physical Review Letters*, **49**, 1804-1807. https://doi.org/10.1103/physrevlett.49.1804

[33] Fritz, T. (2010) Quantum Correlations in the Temporal Clauser-Horne-Shimony-Holt (CHSH) Scenario. *New Journal of Physics*, **12**, Article 083055. https://doi.org/10.1088/1367-2630/12/8/083055

[34] Quintino, M.T., Uola, R., Budroni, C. and Gühne, O. (2019) Inequivalence of Tem-

poral and Spatial Quantum Correlations. *Physical Review Letters*, **123**, Article 180401.

[35] Costa, A.C.S., Uola, R. and Gühne, O. (2018) Steering Criteria from General Entropic Uncertainty Relations. *Physical Review A*, **98**, Article 050102. https://doi.org/10.1103/physreva.98.050104

[36] Sombillo, D.L. and Galapon, E.A. (2014) Quantum Traversal Time through a Double Barrier. *Physical Review A*, **90**, Article 032115. https://doi.org/10.1103/physreva.90.032115

[37] Clauser, J.F., Horne, M.A., Shimony, A. and Holt, R.A. (1969) Proposed Experiment to Test Local Hidden-Variable Theories. *Physical Review Letters*, **23**, 880-884. https://doi.org/10.1103/physrevlett.23.880

[38] Mostafazadeh, A. (2010) Pseudo-Hermitian Representation of Quantum Mechanics. *International Journal of Geometric Methods in Modern Physics*, **7**, 1191-1306. https://doi.org/10.1142/s0219887810004816

[39] Nakahara, M. (2003) Geometry, Topology and Physics. 2nd Edition, Taylor & Francis.

[40] Frankel, T. (2011) The Geometry of Physics. 3rd Edition, Cambridge University Press. https://doi.org/10.1017/cbo9781139061377

[41] Peruzzo, A., Shadbolt, P., Brunner, N., Popescu, S. and O'Brien, J.L. (2012) A Quantum Delayed-Choice Experiment. *Science*, **338**, 634-637. https://doi.org/10.1126/science.1226719

[42] Ma, X.S., Kofler, J., Qarry, A., Tetik, N., Scheidl, T., Ursin, R., *et al.* (2013) Quantum Erasure with Causally Disconnected Choice. *Proceedings of the National Academy of Sciences*, **110**, 1221-1226. https://doi.org/10.1073/pnas.1213201110

[43] Vedovato, F., Agnesi, C., Schiavon, M., Dequal, D., Calderaro, L., Tomasin, M., *et al.* (2017) Extending Wheeler's Delayed-Choice Experiment to Space. *Science Advances*, **3**, e1701180. https://doi.org/10.1126/sciadv.1701180

[44] Kaiser, F., Coudreau, T., Milman, P. and Tanzilli, S. (2020) Quantum Delayed-Choice Experiment with Entanglement. *Science Advances*, **6**, eaaz4204.

[45] Budroni, C. and Emary, C. (2014) Temporal Quantum Correlations and Leggett-Garg Inequalities in Multilevel Systems. *Physical Review Letters*, **113**, Article 050401. https://doi.org/10.1103/physrevlett.113.050401

[46] Kofler, J. and Brukner, Č. (2007) Classical World Arising Out of Quantum Physics under the Restriction of Coarse-Grained Measurements. *Physical Review Letters*, **99**, Article 180403. https://doi.org/10.1103/physrevlett.99.180403

[47] Emary, C., Lambert, N. and Nori, F. (2014) Leggett-Garg Inequalities. *Reports on Progress in Physics*, **77**, Article 016001. https://doi.org/10.1088/0034-4885/77/1/016001

Appendix A—Possible Experimental Test of the Internal Coherence Parametrisation

This appendix outlines an interferometric protocol that could test the operational relevance of the configuration-dependent parameter τ introduced in the complex-time model. The aim is to compare the predictions of standard quantum mechanics—including classical environmental decoherence—with those of the internal parametrisation of coherence used in the main text.

A.1. Two Competing Descriptions

Consider a Mach-Zehnder interferometer fed with single photons. After the first beam splitter (BS1), the state is

$$|\psi\rangle = \frac{1}{\sqrt{2}}\left(|A\rangle + \mathrm{e}^{i\phi}|B\rangle\right), \tag{55}$$

with ϕ a controllable phase.

Standard model. Each path interacts differently with an environment E:

$$A|e_0\rangle \to A|e_A\rangle, \quad B|e_0\rangle \to B|e_B\rangle, \tag{56}$$

yielding the visibility

$$\mathcal{V}_{\mathrm{std}} = \left|\langle e_A | e_B\rangle\right|. \tag{57}$$

Complex-time model. The accumulated phase is parametrised by $\mathcal{T} = t - i\tau$, giving

$$\mathcal{V}_{\mathrm{cplx}} = \exp\left(-\Gamma_{\mathrm{eff}}|\Delta\tau|\right). \tag{58}$$

A.2. Interferometer with Two Delayed Choices

We consider two independent late choices:

- a setting $x \in \{x_1, x_2\}$ modifying one arm (phase shifter, EOM, or controlled dephasing);
- a setting $y \in \{y_1, y_2\}$ modifying the final recombination (presence of BS2 or additional phase).

Both choices are made after BS1 and can be causally separated using long fibres and fast modulators, as in modern delayed-choice experiments [41]-[44]. For each pair (x, y), the visibility $\mathcal{V}(x, y)$ is measured.

A.3. Standard Visibility Structure

In the standard model,

$$\mathcal{V}_{\mathrm{std}}(x, y) = \left|\langle e_A(x, y) | e_B(x, y)\rangle\right|, \tag{59}$$

implying:

- $0 \le \mathcal{V}_{\mathrm{std}} \le 1$,
- monotonic decay under increasing noise,
- convexity under statistical mixing.

A.4. Complex-Time Model and Temporal Correlations

In the complex-time model,

$$\mathcal{V}_{\text{cplx}}(x,y)=\exp\left[-\Gamma_{\text{eff}}\left|\Delta\tau(x,y)\right|\right]. \tag{60}$$

Define the temporal correlation

$$C(x,y)=2\mathcal{V}(x,y)-1, \tag{61}$$

and the CHSH-type combination

$$S=C(x_1,y_1)+C(x_1,y_2)+C(x_2,y_1)-C(x_2,y_2). \tag{62}$$

Classical one-dimensional temporal models satisfying macrorealism and non-invasive measurability obey the Leggett-Garg bound [22] and, more generally, the temporal CHSH bound $|S|\le 2$ [46] [47].

The configuration-dependent parametrisation introduced by the complex-time model departs from these assumptions and allows, in principle, values $S>2$ within the same operational protocol, consistent with recent analyses of temporal correlations and steering [33]-[36].

A.5. Experimental Orders of Magnitude

Amplitude of τ. For a visible photon ($E\simeq 1$ eV),

$$|\Delta\tau|\sim\frac{\hbar}{E}|\ln\mathcal{V}|\sim 3\times10^{-17}\ \text{s}. \tag{63}$$

Values

$$R\sim 10^{-16}\text{-}10^{-15}\ \text{s} \tag{64}$$

are sufficient for measurable variations.

Visibility precision. Fibre interferometers routinely achieve

$$\delta\mathcal{V}\sim 10^{-3}\text{-}10^{-2}. \tag{65}$$

Control elements.

- EOM: $f_{\text{EOM}}\sim 1\text{-}10$ GHz, $\Delta t_{\text{switch}}\sim 10^{-10}\text{-}10^{-9}$ s;
- fibres: $L\sim 100$ m - 1 km, $\Delta t_{\text{fib}}\sim 0.5\text{-}5$ μs;
- fast controllers: $\Delta t_{\text{ctrl}}\sim 1\text{-}10$ ns.

These orders of magnitude indicate that:

1) variations of τ of order 10^{-17} - 10^{-16} s are detectable;

2) causally separated delayed choices are feasible with current technology;

3) the required values of R are compatible with experimental exploration.

A.6. CHSH Bound in a Standard Model

In a one-dimensional time model,

$$\mathcal{V}_{\text{std}}(x,y)=\int d\lambda\, p(\lambda)v(x,y,\lambda),\quad v\in[0,1]. \tag{66}$$

Setting $c=2v-1\in[-1,1]$, the combination

$$S(\lambda)=c_{11}+c_{12}+c_{21}-c_{22} \tag{67}$$

satisfies $\left|S(\lambda)\right| \le 2$, hence

$$\left|S_{\text{std}}\right| \le 2. \tag{68}$$

In the complex-time model,

$$\mathcal{V}(x,y) = \exp\left[-\Gamma_{\text{eff}} \left|\Delta\tau(x,y)\right|\right], \tag{69}$$

nonlinear dependencies of $\Delta\tau$ allow values $S > 2$, indicating that real-time evolution alone cannot capture the full structure of coherence.

Supplementary Materials

The following supporting information can be downloaded at: [https://doi.org/10.4236/jqis.2026.162010]. Supplementary Material S1: Monte Carlo procedure and analytical calculations supporting Section 8 of the main text.

A. Overview

This Supplementary Material provides additional numerical and analytical details supporting the results presented in Sec. 8 of the main text. In particular, we give the full Monte Carlo procedure used to evaluate the visibility

$$\mathcal{V} = \exp\left(-\Gamma_{\text{eff}}|\tau|\right)$$

and compare the numerical statistics with the exact analytical prediction. No supplementary figures are required; all results refer directly to **Figure 1** and **Figure 2** of the main text.

B. Supplementary Note 1: Monte Carlo Procedure

B.1. Sampling Procedure

We simulate $N = 10^5$ realisations of the internal rotation angle $\theta \sim \mathcal{U}(0, 2\pi)$, as assumed in Sec. 8. For each realisation, the imaginary-time coordinate is

$$\tau = R\sin\theta, \tag{S1}$$

with $R = 50$ fs, and the corresponding visibility is

$$V = \exp\left(-\Gamma_{\text{eff}}|\tau|\right), \tag{S2}$$

where $\Gamma_{\text{eff}} = 0.3$ THz is the operational dephasing rate defined in Sec. 4 of the main text.

B.2. Randomness and Reproducibility

Random numbers are generated with a fixed seed (seed = 12345) to ensure full reproducibility. All simulations use standard pseudo-random number generators with uniform sampling of θ.

B.3. Monte Carlo Results

A Monte Carlo simulation with $N = 10^5$ realisations yields:

$$\langle V \rangle_{\text{MC}} = 0.04263. \tag{S3}$$

$$\text{Std}(V) = 0.13915. \tag{S4}$$

$$V_{\min} = 3.06\times10^{-7}, \quad V_{\max} = 0.99967. \tag{S5}$$

These values are dominated by statistical fluctuations of order $1/\sqrt{N} \approx 3\times10^{-3}$, reflecting the fact that the true visibility is extremely small for the parameters considered.

C. Supplementary Note 2: Analytical Prediction

The exact analytical average visibility is

$$\langle V \rangle_{\text{exact}} = \frac{1}{2\pi}\int_0^{2\pi} e^{-\Gamma_{\text{eff}} R|\sin\theta|} d\theta = \frac{2}{\pi} K_0\left(\Gamma_{\text{eff}} R\right), \tag{S6}$$

where K_0 is the modified Bessel function of the second kind.

For the present parameters,

$$\Gamma_{\text{eff}} R = 15, \quad K_0(15) \approx 3.7 \times 10^{-7},$$

yielding

$$\langle V \rangle_{\text{exact}} \approx 2.35 \times 10^{-7}. \tag{S7}$$

The Monte Carlo estimate is therefore consistent with the analytical prediction: the true visibility is several orders of magnitude smaller than the sampling noise, explaining why the empirical mean is dominated by fluctuations. This behaviour matches the exponential suppression shown in **Figure 1** of the main text.

In addition, the sampling relation $\tau = R\sin\theta$ used here corresponds directly to the geometric dependence illustrated in **Figure 2** of the main text, where $\Delta\tau = R\left(\sin\theta_B - \sin\theta_A\right)$. The Monte Carlo procedure thus provides a numerical counterpart to both analytical curves presented in **Figure 1** and **Figure 2**.